Proceedings of CONF-APMM 2026 Symposium: Quantum Communication and Model Simulation
DOI: 10.54254/2753-8818/2026.GL36171

Bandgap Engineering of Si-Ge-Sn Alloys for CMOS-Compatible Infrared Optoelectronic Devices

Rongbin Yuan

School of Information Engineering, Guangdong University of Technology, Guangzhou, China
yuanrongbin@mails.gdut.edu.cn

Abstract. Si-Ge-Sn alloys provide a promising group-IV platform for integrating tunable infrared functions with complementary metal–oxide–semiconductor (CMOS) technology. This review evaluates how epitaxial growth, alloy composition, strain, and heterostructure design influence the electronic structure and device performance of GeSn and SiGeSn materials. Representative experimental and theoretical studies are compared in terms of growth strategy, band alignment, optical response, and reported photodetector and laser characteristics. The reviewed results show that Sn incorporation narrows the GeSn bandgap and lowers the Γ conduction-band valley relative to the L valley, whereas Si alloying mainly adjusts lattice matching and band offsets. Tensile strain and quantum confinement can further enhance direct-gap behavior and carrier overlap. These mechanisms have enabled short-wave infrared photodetectors with multi-gigahertz bandwidth, room-temperature optically pumped GeSn lasers, and electrically pumped SiGeSn/GeSn multiple-quantum-well lasers at cryogenic temperatures. However, device performance remains limited by defect-assisted recombination, dark current, shallow carrier barriers, self-heating, and process non-uniformity. The available evidence therefore indicates that practical Si-Ge-Sn infrared photonics will require the coordinated optimization of epitaxial quality, strain, band alignment, interfaces, and device architecture rather than the independent maximization of Sn content.

Keywords: Si-Ge-Sn alloys, bandgap engineering, strain engineering, infrared photodetectors, quantum wells

1. Introduction

The growing use of silicon photonics in sensing, imaging, and optical communication has increased the demand for infrared components that can be integrated directly with silicon-based circuits. III-V semiconductors already provide efficient emitters and detectors, but their incorporation usually requires bonding, material transfer, or growth processes that are not native to the silicon platform. GeSn and SiGeSn offer a different route. Both belong to the group-IV material family, and their band structures can be adjusted through composition and strain over wavelength ranges that are relevant to infrared detection and emission [1]. This combination of spectral tunability and compatibility with silicon processing has made Si-Ge-Sn alloys an important candidate for integrated infrared photonics.

© 2026 The Authors. This is an open access article distributed under the terms of the Creative Commons Attribution License 4.0 (https://creativecommons.org/licenses/by/4.0/).

DOI: 10.54254/2753-8818/2026.GL36171

The usefulness of the material system, however, cannot be judged from its nominal bandgap alone. Sn lowers the GeSn bandgap and changes the relative positions of the Γ and L conduction-band valleys, but the final electronic structure also depends on residual strain and alloy disorder. Si has a different function: it modifies the lattice parameter and redistributes the conduction- and valence-band offsets. Defects, interface roughness, and compositional fluctuations further influence carrier lifetime, transport, and optical transitions. Consequently, a composition that appears favorable in a band calculation may perform poorly after epitaxial growth or device fabrication. The central issue is therefore the extent to which composition, strain, crystal quality, and heterostructure design can be controlled at the same time.

The discussion in this article is based on a comparative reading of recent theoretical calculations, optical characterization studies, and experimental device reports. Rather than placing all results in a single chronological sequence, the literature is examined according to the physical link between material preparation and device behavior. The first part considers the growth of GeSn and SiGeSn, with particular attention to Sn segregation, metastability, strain relaxation, and interface defects. The second part deals with the electronic mechanisms that underlie bandgap engineering, including the unequal shifts of the Γ and L valleys, Si-dependent band alignment, strain-induced changes in directness, and quantum confinement in SiGeSn/GeSn wells. The final part compares reported photodetectors and lasers through measurable quantities such as cutoff wavelength, responsivity, detectivity, bandwidth, threshold current, and operating temperature.

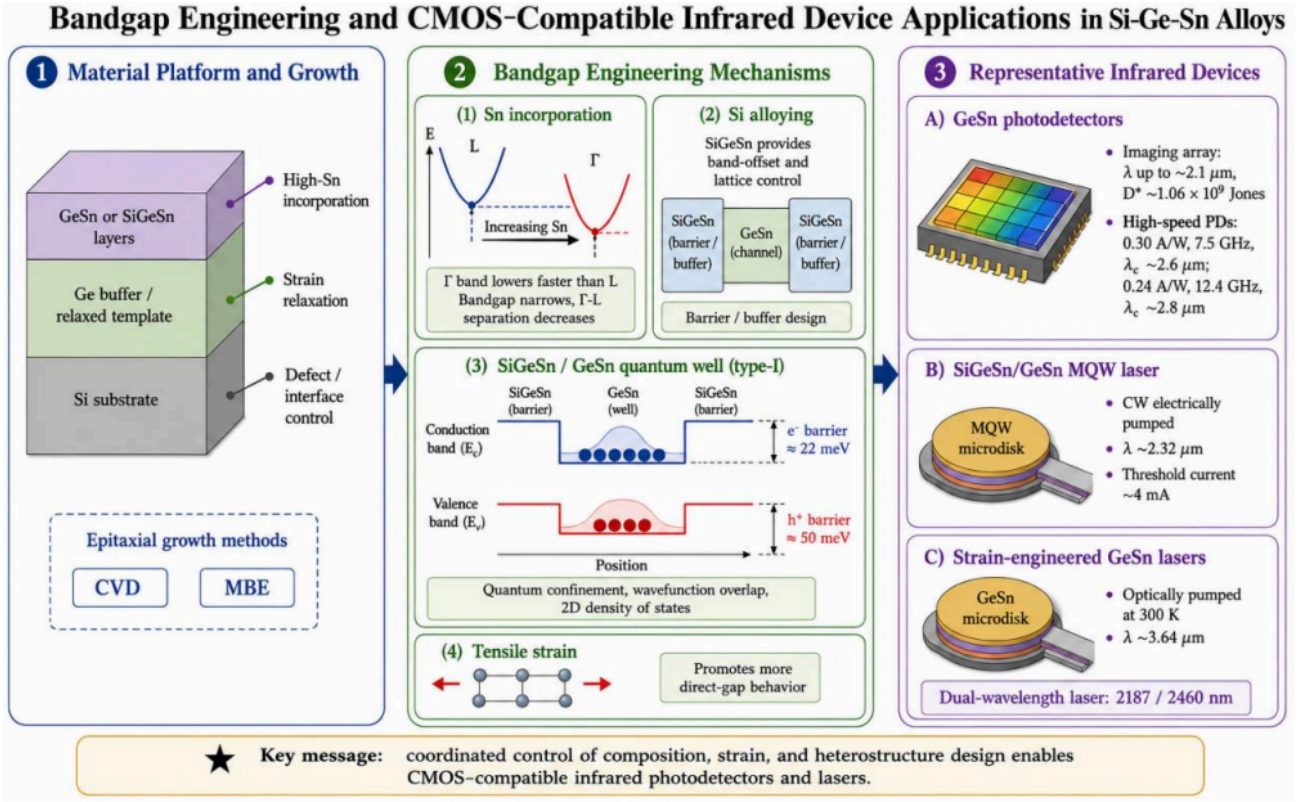

Figure 1. Schematic overview of the material platform, bandgap engineering mechanisms, and representative CMOS-compatible infrared optoelectronic devices based on Si-Ge-Sn alloys

The purpose of this organization is to determine where the main limitations of Si-Ge-Sn devices actually arise. Some originate in the alloy itself, whereas others are introduced by relaxation,

DOI: 10.54254/2753-8818/2026.GL36171

interfaces, contacts, carrier leakage, or thermal effects. Distinguishing these contributions is necessary before improvements in material composition can be translated into better device performance. Figure 1 summarizes this connection: epitaxial growth establishes the available material quality and strain state, bandgap engineering defines the electronic and optical transitions, and the device structure determines how effectively carriers are generated, confined, injected, or collected. On this basis, the article evaluates both the present potential of Si-Ge-Sn infrared devices and the conditions required for their further integration with CMOS-compatible photonic systems.

2. Growth of Si-Ge-Sn alloys and material challenges

2.1. GeSn and SiGeSn material system

GeSn and SiGeSn do not play identical roles in infrared heterostructures. GeSn is commonly selected as the absorbing or gain layer, whereas SiGeSn is more often used to shape the surrounding band profile. In this material system, GeSn is usually employed as the active absorption or gain medium because Sn incorporation reduces the bandgap of Ge-based alloys and extends the optical response toward longer infrared wavelengths. SiGeSn, by contrast, provides an additional design parameter through Si alloying. Although the introduction of Si can enlarge the alloy bandgap, it also enables lattice-constant adjustment, band-offset control, and barrier-layer engineering. Therefore, SiGeSn is particularly useful in buffer layers, carrier-confinement structures, and GeSn-based quantum wells.

A useful way to understand the Si-Ge-Sn system is to regard GeSn and SiGeSn as complementary materials rather than members of a single alloy family with identical functions. GeSn generally serves as the narrow-bandgap active region responsible for infrared absorption or optical gain, whereas SiGeSn is mainly used to adjust lattice compatibility, band offsets, and carrier confinement. This division of roles is particularly important in heterostructure design. In photodetectors, the GeSn layer determines much of the absorption range, while the surrounding SiGeSn layers can modify carrier transport and leakage. In emitters and lasers, GeSn provides the radiative transition or gain medium, whereas SiGeSn barriers help retain electrons and holes in the active region. The design is nevertheless subject to clear trade-offs. Increasing the Sn content extends the spectral response and promotes a more direct bandgap, but it also increases the tendency toward segregation, strain relaxation, and defect formation. Increasing the Si content can strengthen the heterostructure barrier and improve lattice control, but it may also widen the bandgap and move the structure away from the desired long-wavelength response. The practical value of Si-Ge-Sn heterostructures therefore depends on balancing spectral range, carrier confinement, strain stability, and crystalline quality.

2.2. Epitaxial growth methods

Epitaxial growth must incorporate Sn substitutionally into a diamond-like lattice far beyond its equilibrium solubility. This requirement explains the reliance on non-equilibrium, low-temperature growth. Chemical vapor deposition (CVD) is attractive for wafer-scale processing and has been widely used on Ge-buffered Si, whereas molecular beam epitaxy (MBE) offers tighter control of flux and interface sequence. In CVD, precursor chemistry, temperature, pressure, and growth rate determine whether Sn is incorporated or rejected at the surface. The reported growth window is narrow: conditions that favor higher Sn content can also reduce surface mobility and roughen the film [2].

DOI: 10.54254/2753-8818/2026.GL36171

MBE is particularly useful when abrupt composition changes are required, as in quantum wells, but it does not remove the underlying thermodynamic limitation. Low substrate temperature suppresses Sn desorption and precipitation, yet it also limits adatom diffusion. The result is a recurring compromise between composition and crystalline order. Similar compromises appear in CVD, where a process that raises Sn uptake may also promote defects or compositional grading. For this reason, growth conditions should be evaluated together with strain and optical data rather than by nominal alloy composition alone [3].

Buffer design provides a second level of control. Direct deposition on Si would combine large lattice and thermal mismatches, so most structures employ a Ge virtual substrate, a graded GeSn buffer, or another partially relaxed template. These layers reduce the mismatch seen by the active region, but they can also transmit threading dislocations or introduce additional interfaces. In ternary SiGeSn, control becomes more demanding because the arrival and incorporation rates of three elements must be balanced without losing phase stability. The practical objective is not complete relaxation at any cost; it is a reproducible strain state with an acceptably low defect density.

2.3. Challenges of Sn incorporation and strain relaxation

Sn incorporation is difficult for both chemical and structural reasons. The equilibrium solubility of Sn in Ge is very low, and the larger Sn atom produces substantial local strain. As the Sn supply is increased, substitutional incorporation competes with surface segregation, clustering, and phase separation. These processes may appear as surface roughness, vertical composition gradient, or Sn-rich segregated regions and precipitates. Yet high Sn content is precisely what is sought for bandgap reduction. The growth problem is therefore defined by a narrow operating window in which Sn is retained in the lattice without allowing the crystal quality to collapse.

The strain state adds another constraint. A GeSn layer grown coherently on Ge is generally under biaxial compression because its relaxed lattice constant is larger. Compression changes the Γ-L valley separation and can partly cancel the band-structure advantage expected from the added Sn. Relaxation can recover a more favorable electronic structure, but plastic relaxation introduces misfit and threading dislocations. In other words, a more relaxed layer is not necessarily a better optical layer. The relevant outcome depends on how the strain is released and on the defect network produced during that release.

Several strategies address this balance. Step-graded buffers distribute the mismatch across multiple interfaces, while released membranes and microdisks permit elastic relaxation after growth. Local tensile strain can also be introduced with external stressors, and pulsed laser melting has been explored as a post-growth treatment. Each approach changes more than one variable. Release structures improve the strain state but complicate thermal management and fabrication; graded buffers improve lattice accommodation but increase thickness and dislocation-propagation paths. A scalable process must therefore combine strain control with surface uniformity and low-defect interfaces.

2.4. Effects of defects on optical and electrical properties

Defects determine how closely the measured material follows its calculated band structure. Vacancies, impurity complexes, threading dislocations, interface states, and local composition fluctuations introduce defect states or structural perturbations that alter carrier transport, recombination, and optical transitions. Their effects are not identical: some shorten the minority-carrier lifetime, some assist generation under reverse bias, and others scatter carriers or broaden

DOI: 10.54254/2753-8818/2026.GL36171

optical transitions. In quantum wells, interface roughness and interdiffusion also change the local well width and barrier height [4].

These effects are especially severe in narrow-gap GeSn. In a photodiode, defect-assisted generation adds to the intrinsic thermal current and can dominate the noise floor. In an emitter, the same defects divert carriers away from radiative recombination, raising the excitation or injection required for optical gain. This explains why two samples with similar Sn content and nominal strain may show very different responsivity, luminescence intensity, or lasing threshold. Material quality is therefore part of the electronic design, not merely a growth-quality label.

Interfaces become more important as the structure becomes more complex. A SiGeSn/GeSn multiple-quantum-well stack contains many opportunities for intermixing, roughness, and accumulated elastic energy. Even modest interdiffusion can smooth the intended band discontinuity, while strain accumulation may trigger relaxation in later periods. Consequently, composition, thickness, and interface abruptness must be checked experimentally rather than assumed from the growth recipe. This requirement links structural characterization directly to any interpretation of band offsets and optical transitions.

3. Bandgap engineering mechanisms in Si-Ge-Sn alloys

3.1. Sn-composition-dependent bandgap tuning

Pure Ge has an indirect fundamental gap because the L conduction minimum lies below the Γ minimum. Alloying with Sn lowers both valleys, but the Γ edge moves more rapidly. As the Sn fraction increases, the Γ minimum approaches the L minimum and, at sufficiently high Sn content under suitable strain conditions, may fall below it. GeSn can therefore become direct or nearly direct when the Γ valley becomes the lowest conduction-band minimum. This unequal valley shift, rather than bandgap narrowing by itself, is the key reason GeSn is considered for group-IV light emission.

No single Sn percentage defines the crossover in every sample. The predicted value changes with strain, temperature, alloy disorder, and the parameters adopted in density-functional, empirical-pseudopotential, or k·p calculations. Strong bowing also makes a linear interpolation between Ge and α-Sn unreliable. Atomistic disorder adds a further complication because the same average composition can contain different local bonding environments.

Optical measurements generally follow the expected composition trend: the absorption edge and photoluminescence peak move to lower energy as the Sn fraction rises. Their interpretation still requires care. Photoluminescence intensity depends on excitation, carrier density, defects, and collection geometry, so stronger emission is not by itself proof of a direct fundamental gap. A more convincing analysis combines absorption or photoreflectance with temperature-dependent luminescence, strain measurements, and a composition-aware band model [5].

3.2. Si alloying and band alignment control

Si changes the design space in a different way from Sn. It usually increases the alloy bandgap and reduces the relaxed lattice constant. When the Si and Sn fractions are varied together, the bandgap and lattice parameter can therefore be adjusted to some extent independently. This is valuable in heterostructures, where the active GeSn layer may require both a wider-gap surrounding material and a manageable lattice mismatch.

The distribution of the discontinuity between the conduction and valence bands is as important as the total gap difference. Type-I alignment places the lowest electron and hole states in the same

DOI: 10.54254/2753-8818/2026.GL36171

GeSn region, whereas type-II alignment separates them spatially. Type-I alignment favors electron–hole wavefunction overlap, whereas type-II alignment reduces their spatial overlap and modifies carrier lifetime and transport. Neither label alone predicts a useful device, because injection and extraction also depend on the actual barrier heights and on the contacts.

Band offsets are often estimated with model-solid, deformation-potential, atomistic, or multiband k·p approaches, but the results remain sensitive to strain and bowing assumptions. Direct measurement is therefore valuable. Internal-photoemission experiments on a SiGeSn/GeSn quantum well reported type-I alignment with effective barriers of 22 ± 2 meV for electrons and 50 ± 2 meV for holes [6]. The asymmetry is significant: holes were more strongly confined, while the relatively shallow electron barrier leaves greater scope for thermal escape.

3.3. Strain engineering and direct-bandgap transition

Strain modifies the band edges through deformation-potential coupling. Its hydrostatic component shifts the average gap, while biaxial or uniaxial components alter the relative positions of the Γ and L valleys. For a fixed Sn composition, residual compression generally makes the material less direct than its relaxed counterpart. Tensile strain has the opposite tendency and can reduce the Γ valley relative to L.

The valence bands respond as well. Strain separates the heavy-hole and light-hole states, changing the density of states, optical polarization, and allowed transition strengths. This is why samples with similar composition can show different emission spectra even before differences in defect density are considered. Composition-only bandgap plots are therefore useful as a first approximation, but they are incomplete for epitaxial layers.

Raman spectroscopy and high-resolution X-ray diffraction provide complementary measures of strain and relaxation, which can then be compared with absorption and photoluminescence. A released GeSn microbridge with approximately 1.23% uniaxial tensile strain showed an emission redshift of roughly 500 nm together with an order-of-magnitude enhancement of direct-gap luminescence [7]. The observation illustrates the scale of the strain effect, while also showing why mechanical geometry must be included when optical data from patterned structures are interpreted.

3.4. Quantum confinement in SiGeSn/GeSn heterostructures

A GeSn layer confined between wider-gap SiGeSn barriers forms a finite quantum well. Quantum confinement reorganizes the three-dimensional bulk states into quasi-two-dimensional electron and hole subbands. Their quantized energies depend on the well width, effective masses, barrier heights, and strain, while carrier motion within the plane of the well remains continuous. Thinner wells generally raise the confinement energy, shifting the interband transition above the bulk GeSn gap.

For type-I alignment, the electron and hole envelope functions are concentrated in the same layer, which increases their spatial overlap. The confinement is nevertheless finite. If the electron barrier is shallow, part of the wavefunction extends into the SiGeSn barrier, reducing localization and increasing sensitivity to temperature. The well also changes the density of states from a three-dimensional continuum to a sequence of two-dimensional steps.

The corresponding optical transition energy includes contributions from the well bandgap, the electron and hole confinement energies, and the exciton binding energy. Its strength depends on both the envelope-function overlap and the underlying Bloch-state matrix element. These quantities describe the intrinsic physics of the heterostructure. Device gain, responsivity, threshold current, and

DOI: 10.54254/2753-8818/2026.GL36171

modulation bandwidth additionally depend on injection, contacts, losses, and cavity geometry, and are therefore treated separately in Section 4.

4. CMOS-compatible infrared optoelectronic device applications

4.1. GeSn and SiGeSn infrared photodetectors

GeSn photodetectors have been demonstrated as p-type-intrinsic-n-type (p-i-n) photodiodes, heterojunction photodiodes, waveguide detectors, and imaging arrays. Their principal metrics are responsivity, external quantum efficiency, specific detectivity, dark-current density, cutoff wavelength, and electrical bandwidth.

A 2024 CMOS-compatible demonstration used a 4 × 4 GeSn p-i-n heterojunction pixel array monolithically integrated on Si. With 6.3% Sn in the absorbing layer, it extended detection to approximately 2.1 μm and achieved a peak specific detectivity of about 1.06×10^9 Jones under uncooled, self-powered operation [8]. The array also produced short-wave infrared images.

A 2022 Si-integrated GeSn photodiode achieved a peak room-temperature responsivity of approximately 0.30 A/W, a cutoff wavelength of 2.6 μm, and a 3-dB bandwidth of 7.5 GHz at 5 V reverse bias [9]. A later all-GeSn vertical p-i-n device achieved 12.4 GHz bandwidth, 0.24 A/W responsivity, and a 2.8 μm cutoff [10]. These results show that performance depends on capacitance, series resistance, junction design, and optical coupling as well as absorber bandgap.

4.2. SiGeSn/GeSn quantum-well devices

A representative SiGeSn/GeSn device is the six-period multiple-quantum-well microdisk laser reported in 2024. It emitted near 2.32 μm and reached a threshold current of approximately 4 mA [11]. Its linewidth was about 15 GHz, and continuous-wave lasing was maintained up to approximately 35 K. With shorter pulses and reduced heating, lasing was observed up to about 70 K.

Compared with an earlier SiGeSn/GeSn/SiGeSn double-heterostructure microdisk, the multiple-quantum-well device reduced the threshold-current density by about eight times despite using less total gain material. Under comparable under-etch conditions, the reduction was approximately twelvefold [11]. The improvement reflects the combined effects of carrier confinement, two-dimensional density of states, junction injection, and cavity design.

The device remained limited by self-heating and thermal carrier escape. Future structures require deeper electron barriers, lower-resistance contacts, improved heat extraction, and optimized well and barrier thicknesses.

4.3. GeSn and SiGeSn lasers for silicon photonics

Laser performance is usually compared using wavelength, threshold pump density or current, maximum operating temperature, linewidth, and output power. Strain-engineered $Ge_{0.86}Sn_{0.14}$ microdisks demonstrated optically pumped lasing at 300 K. With approximately 0.8-1% tensile strain from a silicon-nitride stressor, the device emitted near 3.64 μm with a threshold pump density of approximately 550 kW/cm^2 [12].

A 2023 all-group-IV laser containing bulk GeSn and a SiGeSn/GeSn multiple-quantum-well region produced simultaneous lasing at approximately 2187 and 2460 nm. Dual-wavelength lasing began at about 420 kW/cm^2 [13]. This demonstrated wavelength multiplexing in a monolithically grown group-IV structure, although the high pump density indicated substantial losses.

DOI: 10.54254/2753-8818/2026.GL36171

These results show progress in wavelength coverage, operating temperature, and electrical injection. However, no reported device has yet combined room-temperature continuous-wave electrical pumping, low threshold, high output power, and wafer-scale uniformity.

4.4. Current device limitations and future directions

Current Si-Ge-Sn devices have achieved uncooled imaging, detector bandwidths above 10 GHz, room-temperature optically pumped lasing, and cryogenic electrically pumped continuous-wave lasing. Their performance is still restricted by dark current, defect-assisted recombination, carrier leakage, self-heating, contact resistance, and device variation.

For photodetectors, future research should emphasize surface passivation, mesa-edge isolation, lower-defect buffers, optimized intrinsic-layer thickness, and barrier-assisted structures. Comparisons should report dark-current density, responsivity, detectivity, and bandwidth under clearly stated wavelength, temperature, bias, and optical-power conditions.

For lasers, the main goals are to suppress defect-related recombination, increase the Γ-L energy separation, deepen quantum-well barriers, reduce electrical resistance, and improve thermal management. A 2024 analysis estimated that defect-related recombination accounted for 93 ± 5% of the threshold current at 85 K in the investigated device, indicating that defect reduction may be as important as further Sn incorporation [14].

Future work must also move from isolated microdevices toward reproducible wafer-scale arrays and photonic circuits. Uniform composition and strain, compatible thermal budgets, stable contacts, and effective heat removal will be essential. The long-term objective is to achieve room-temperature, continuous-wave, electrically driven devices that can be manufactured reliably on silicon.

5. Conclusion

Several conclusions can be drawn from the studies discussed in this article. First, the infrared properties of Si-Ge-Sn alloys are not controlled by Sn concentration alone. A higher Sn fraction generally narrows the GeSn bandgap and moves the Γ conduction-band valley closer to, or below, the L valley. In an actual epitaxial layer, however, this change may be weakened or enhanced by residual strain, local alloy disorder, and defects. Si incorporation affects the system in another way by changing the relaxed lattice parameter and the conduction- and valence-band offsets. It is therefore particularly useful in SiGeSn barriers surrounding a GeSn active layer. Tensile strain and quantum confinement can further improve direct-gap character and electron-hole overlap, but only when interface degradation, carrier escape, and structural relaxation remain limited.

The device results reflect the same balance. GeSn photodetectors have extended silicon-based detection into the short-wave infrared and have reached multi-gigahertz bandwidths. GeSn microdisks have produced optically pumped lasing at room temperature, while SiGeSn/GeSn multiple-quantum-well devices have demonstrated electrically pumped lasing at lower temperatures. These achievements confirm that the material platform is capable of both detection and emission. They also reveal why progress in band structure does not always produce an equivalent improvement in device performance. Dark current, non-radiative recombination, shallow electron barriers, contact resistance, optical loss, and self-heating may dominate after the material is incorporated into a junction or resonant cavity. The practical conclusion is that the most favorable alloy composition is not necessarily the one that produces the best device.

DOI: 10.54254/2753-8818/2026.GL36171

By separating intrinsic band-structure effects from losses introduced during growth and fabrication, this review provides a clearer basis for interpreting reported performance. The comparison is useful for identifying whether a limitation is mainly associated with the alloy, the strain state, the heterointerface, the electrical junction, or the optical cavity. It also helps to explain why devices with similar Sn contents can exhibit very different responsivities, thresholds, or operating temperatures.

Further development will depend on improvements that address these limitations together. More reproducible low-defect epitaxy is needed across larger wafer areas, and band offsets should be verified experimentally rather than inferred only from composition models. Surface passivation, interface control, lower-resistance contacts, and improved heat removal also require greater attention. The decisive benchmarks will be uniform detector arrays and room-temperature, continuous-wave, electrically pumped lasers with stable performance. Reaching these goals would move Si-Ge-Sn technology beyond individual laboratory demonstrations and toward practical infrared photonic integration on silicon.

References

[1] Moutanabbir, O., Assali, S., Gong, X., O'Reilly, E., Broderick, C. A., Marzban, B., Witzens, J., Du, W., Yu, S.-Q., Chelnokov, A., Buca, D., & Nam, D. (2021). Monolithic infrared silicon photonics: The rise of (Si)GeSn semiconductors. *Applied Physics Letters, 118*(11), 110502. https://doi.org/10.1063/5.0043511

[2] Miao, Y., Wang, G., Kong, Z., Xu, B., Zhao, X., Luo, X., Lin, H., Dong, Y., Lu, B., Dong, L., Zhou, J., Liu, J., & Radamson, H. H. (2021). Review of Si-based GeSn CVD growth and optoelectronic applications. *Nanomaterials, 11*(10), 2556. https://doi.org/10.3390/nano11102556

[3] Kong, Z., Wang, G., Liang, R., Su, J., Xun, M., Miao, Y., Gu, S., Li, J., Cao, K., Lin, H., Li, B., Ren, Y., Li, J., Xu, J., & Radamson, H. H. (2022). Growth and strain modulation of GeSn alloys for photonic and electronic applications. *Nanomaterials, 12*(6), 981. https://doi.org/10.3390/nano12060981

[4] Giunto, A., & Fontcuberta i Morral, A. (2024). Defects in Ge and GeSn and their impact on optoelectronic properties. *Applied Physics Reviews, 11*(4), 041333. https://doi.org/10.1063/5.0218623

[5] Jernigan, G. G., Murphy, J. P., Mahadik, N. A., Grede, A. J., Jackson, E. M., & Nolde, J. A. (2024). Infrared optical properties of SiGeSn and GeSn layers grown by molecular beam epitaxy. *Journal of Vacuum Science & Technology B, 42*(5), 052209. https://doi.org/10.1116/6.0003585

[6] Rudie, J., Tran, H., Zhang, Y., Amoah, S., Acharya, S., Stanchu, H., Mortazavi, M., Morgan, T. A., Forcherio, G. T., Sun, G., Salamo, G. J., Du, W., & Yu, S.-Q. (2025). Study of electronic band alignment in SiGeSn/GeSn quantum well via internal photoemission effect. *Applied Physics Letters, 127*(3), 031102. https://doi.org/10.1063/5.0280475

[7] Burt, D., Zhang, L., Jung, Y., Joo, H.-J., Kim, Y., Chen, M., Son, B., Fan, W., Ikonic, Z., Tan, C. S., & Nam, D. (2023). Tensile strained direct bandgap GeSn microbridges enabled in GeSn-on-insulator substrates with residual tensile strain. *Optics Letters, 48*(3), 735–738. https://doi.org/10.1364/OL.476517

[8] Wang, P.-C., Huang, P.-R., Ghosh, S., Bansal, R., Jheng, Y.-T., Lee, K.-C., Cheng, H. H., & Chang, G.-E. (2024). CMOS-compatible self-powered short-wave infrared imagers based on GeSn photodetector arrays. *ACS Photonics, 11*(7), 2659–2666. https://doi.org/10.1021/acsphotonics.4c00374

[9] Atalla, M. R. M., Assali, S., Koelling, S., Attiaoui, A., & Moutanabbir, O. (2022). High-bandwidth extended-SWIR GeSn photodetectors on silicon achieving ultrafast broadband spectroscopic response. *ACS Photonics, 9*(4), 1425–1433. https://doi.org/10.1021/acsphotonics.2c00260

[10] Atalla, M. R. M., Lemieux-Leduc, C., Assali, S., Koelling, S., Daoust, P., & Moutanabbir, O. (2024). Extended short-wave infrared high-speed all-GeSn PIN photodetectors on silicon. *APL Photonics, 9*(5), 056103. https://doi.org/10.1063/5.0197018

[11] Seidel, L., Liu, T., Concepción, O., Marzban, B., Kiyek, V., Spirito, D., Schwarz, D., Benkhelifa, A., Schulze, J., Ikonic, Z., Hartmann, J.-M., Chelnokov, A., Witzens, J., Capellini, G., Oehme, M., Grützmacher, D., & Buca, D. (2024). Continuous-wave electrically pumped multi-quantum-well laser based on group-IV semiconductors. *Nature Communications, 15*, 10502. https://doi.org/10.1038/s41467-024-54873-z

[12] Buca, D., Bjelajac, A., Spirito, D., Concepción, O., Gromovyi, M., Sakat, E., Lafosse, X., Ferlazzo, L., von den Driesch, N., Ikonic, Z., Grützmacher, D., Capellini, G., & El Kurdi, M. (2022). Room temperature lasing in GeSn

DOI: 10.54254/2753-8818/2026.GL36171

microdisks enabled by strain engineering. *Advanced Optical Materials, 10*(22), 2201024. https://doi.org/10.1002/adom.202201024

[13] Abernathy, G., Ojo, S., Said, A., Grant, J. M., Zhou, Y., Stanchu, H., Du, W., Li, B., & Yu, S.-Q. (2023). Study of all-group-IV SiGeSn mid-IR lasers with dual wavelength emission. *Scientific Reports, 13*, 18515. https://doi.org/10.1038/s41598-023-45916-4

[14] Ellis, A. R., Duffy, D. A., Marko, I. P., Acharya, S., Du, W., Yu, S.-Q., & Sweeney, S. J. (2024). Challenges for room temperature operation of electrically pumped GeSn lasers. *Scientific Reports, 14*, 10318. https://doi.org/10.1038/s41598-024-60686-3